Removal of Lead Ions by Hydroxyapatite Prepared from the Egg Shell

S. Meski,* S. Ziani, and H. Khireddine

Faculté de Technologie, Département de Génie des Procédés, Laboratoire de Génie de l'Environnement, Université de Bejaia, Algérie

Carbonate hydroxyapatite (CHAP) was synthesized from domestic hen egg shells. The obtained CHAP was characterized by X-ray diffraction (XRD) and Fourier transform infrared spectroscopy and investigated as metal adsorption for Pb^{2+} from aqueous solutions. The effect of various parameters on the adsorption process such as contact time, solution pH, and temperature was studied to optimize the conditions for maximum adsorption. The results showed that the removal efficiency of Pb^{2+} by carbonate hydroxyapatite calcined at 600 °C (CHAPF) reached 99.78 %, with an initial Pb^{2+} concentration of 200 $mg \cdot L^{-1}$, pH = 3, and a solid/liquid ratio of 1 $g \cdot L^{-1}$. The equilibrium removal process of lead ions by CHAPF foam at pH = 3 was well described by the Langmuir isotherm model, with a maximum adsorption capacity of 500 $mg \cdot g^{-1}$ at (25 and 35) °C. The removal mechanism of Pb^{2+} by the CHAPF varies, depending on the initial concentration of lead in the aqueous solution: the dissolution of CHAPF and precipitation of hydropyromorphite ($Pb_{10}(PO_4)_6(OH)_2$) is dominant at low concentration [(20 to 200) $mg \cdot L^{-1}$], and the adsorption mechanism of Pb^{2+} on the CHAPF surface and ion exchange reaction between Ca^{2+} of hydroxyapatite and Pb^{2+} in aqueous solution is dominant at high concentration [(500 to 700) $mg \cdot L^{-1}$]. The thermodynamics of the immobilization process indicates an exothermic sorption process of Pb^{2+}.

Introduction

Heavy metals are detrimental to the environment because of their nonbiodegradable and persistent nature.[1] The toxicity of these metals is enhanced through accumulation in living tissues and the food chain.[2] Lead is an important metal from the viewpoint of environmental toxicology.[3] Lead is widely used in sulfuric acid manufacture, petrol refining, halogenation, sulfonation, extraction and condensation, storage batteries, alloys, solder, manufacture of pigments, ceramics, and plastics, and as a consequence, it is often found in wastewaters arising from these processes. Therefore, the elimination of heavy metals from waters and wastewaters is important to protect public health. Many methods have been proposed for heavy metal removal. Chemical precipitation,[4] membrane filtration,[5] ion exchange, and biosorption[6,7] are the most commonly used processes; each has its merits and limitations in application. The major advantages of biosorption include low cost, high efficiency, minimization of chemical or biological sludge, no additional nutrient requirement, possibility of regeneration of the biosorbent, and metal recovery.[8−10] Hydroxyapatite is one of the many adsorbents used. The efficiency of hydroxyapatite depends on factors such as high sorption capacity for heavy metals, low water solubility, and high stability under reducing and oxidizing conditions.

Despite its prolific use in the biomedical domain, hydroxyapatite remains a rather expensive materiel due to the use of high-purity reagents.[11,12] This leads to a search for low-cost materials as alternative adsorbents. It is well-known that hydroxyapatite can be prepared from a variety of raw materials. The most frequently used precursors are animal bones,[13,14] coral,[15] etc.

Important issues in the industrial process are minimization of wastes, recovery of precious materials, and regeneration of wastes and energy. Egg shell waste is widely produced from houses, restaurants, and bakeries. Egg shell has a little developed porosity and pure $CaCO_3$ as an important constituent. In this work, synthesized hydroxyapatite by using egg shell was investigated from the viewpoint of recycling this waste product and minimization of contaminants. Physical and chemical properties of the hydroxyapatite prepared from egg shell were determined, and the potential use of CHAP in the removal of lead was studied.

On the basis of bioresource recycling, the interest of using hen egg shell as an adsorbent has slightly increased in recent years. Zheng et al.[16] studied the sorption of Cd(II) and Cu(II) from aqueous solution by carbonate hydroxyapatite derived from egg shell as a low-cost sorbent, finding that it had a relatively high sorption capacity compared to other sorbents. Liao et al.[17] reported the removal of lead(II) ions from aqueous solution using carbonate hydroxyapatite prepared from egg shell. The study concluded that CHAP could be used as an efficient adsorbent for removal of lead ions from aqueous solution with adsorption capacities of 101 $mg \cdot g^{-1}$ with a 60 min equilibrium time.

Experimental Section

Sorbent Preparation. A carbonate hydroxyapatite sample CHAP was prepared as follows: The egg shells (collected from eggs from a grocery shop) were washed with tap water several times and afterward with distilled water. Then, they were transferred to the oven at 80 °C to dry. The dried egg shells were crushed and milled. The average size of the egg shells was 100 mm. A weight of 33.330 g of egg shell powder was vigorously added to 46.160 mL of nitric acid HNO_3 (d = 1.4, P = 65 %) and stirred at room temperature for 1 h. The reaction that occurred is based on eq 1.

$$CaCO_3 + 2HNO_3 \rightarrow Ca(NO_3)_{2(aq)} + CO_2 + H_2O \quad (1)$$

In the second step, a solution of phosphate was obtained by the dilution of 13.700 mL of H_3PO_4 (d = 1.68, P = 85 %) in

* Corresponding author. E-mail: meskisamira@yahoo.fr.

10.1021/je901070e
Published on Web 07/06/2010

130 mL of distilled water. Subsequently, a solution of H_3PO_4 was slowly added to the solution of $Ca(NO_3)_{2(aq)}$. In all experiments, the pH of $Ca(NO_3)_{2(aq)}$ solution was adjusted to pH 10 using an ammonia solution (NH_4OH, $p = 37$ %), and the suspension was maintained at ebullition temperature for 1 h and at room temperature for 24 h. The reaction proceeded according to eq 2.

$$10Ca(NO_3)_{2(aq)} + 20NH_4OH + 6H_3PO_4 \rightarrow Ca_{10}(PO_4)_6(OH)_2 + 20NH_4NO_3 + 18H_2O \quad (2)$$

Last, the suspension was filtered, dried, and ground into a powder manually (mesh size 0.350 mm) to get the sample. Small amounts of the powder were heated at 600 °C for 3 h and furnace cooled to improve crystallinity and to check the purity.

Characterization of the Sorbents. To study the crystallinity of the prepared samples, powder X-ray diffraction (XRD model PHILLIPS X pert prof, analytical, system MPD) patterns were recorded using Cu Kα radiation at 50 kV and 100 mA. Fourier transform infrared spectroscopic (Shimadzu-8300 IR-TF) analysis was performed to identify the presence of chemical functional groups in the samples, and the point of zero charge (pH_{PZC}) was measured by a batch equilibration technique, with 0.1 N of KNO_3 as an inert electrolyte.[18]

Biosorption Studies. Biosorption equilibrium assays were carried out by adding the dried sorbent in 250 mL of Pb^{2+} solution at the desired concentration and pH at 25 °C in a shaking water bath at 100 rpm. After the required time to reach equilibrium, the suspension was filtered, and the final concentration of Pb^{2+} in solution was measured by using the atomic absorption spectrophotometry technique (Shimadzu AA 6500, air/C_2H_5 gas mixture). The amount of Pb^{2+} adsorbed onto hydroxyapatite q_t (mg·g^{-1}) was calculated by a mass balance relationship

$$q_t = \frac{(C_0 - C_t)V}{m} \quad (3)$$

where q_t (mg·g^{-1}) is the adsorption capacity; C_0 and C_t are the initial and equilibrium concentration (mg·L^{-1}) of lead ions in solution; V (L) is the volume; and m (g) is the weight of the adsorbent.

Results and Discussion

XRD Phase Analysis. The XRD patterns of prepared hydroxyapatite (CHAP) (Figure 1) were found to be similar to that of a heat-treated sample at 600 °C (CHAPF) exhibiting peaks corresponding to hydroxyapatite (JCPDS 9-432) with no secondary phases indicating that the synthesized hydroxyapatite was pure. It was also observed that the crystallinity of the hydroxyapatite powders increased with temperature of calcination. The hydroxyapatite powders calcined at 600 °C (CHAPF) showed well-defined broad crystalline peaks.

FTIR Analysis. Fourier transform infrared (FT-IR) analysis was performed to identify the presence of chemical functional groups in the samples. IR spectra of the CHAP powders before and after calcinations at 600 °C are shown in Figure 2.

In general, the FT-IR spectra of the carbonate hydroxyapatite (CHAP) and those calcined at 600 °C (CHAPF) have intense peaks at a frequency level of (3600 to 3300) cm^{-1}, representing −OH stretching.[19] The peak between (1450 to 1380) cm^{-1} and 1630 cm^{-1} corresponds to the carbonate CO_3^{2-} mode.[20] The

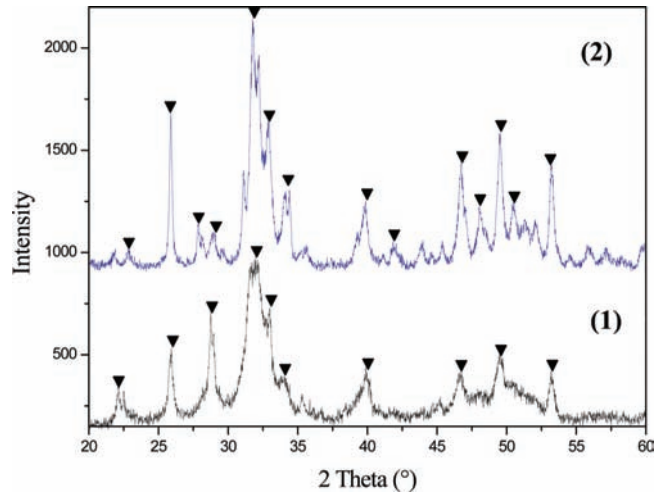

Figure 1. XRD patterns of CHAP (1) and CHAPF (2). Triangle, hydroxyapatite.

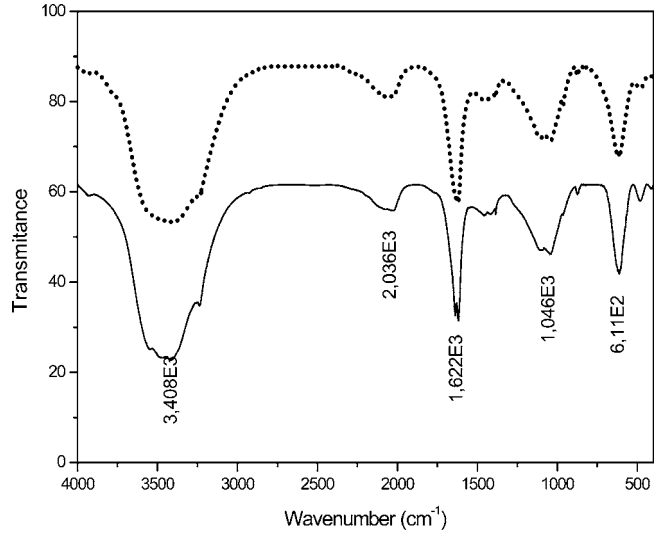

Figure 2. FTIR spectra of —, CHAP and - - -, CHAPF.

band at 870 cm^{-1} could be assigned to the HPO_4^{2-} group.[20,21] In addition, the bands between (2210 and 1950) cm^{-1} and (1046 and 486) cm^{-1} are relative to PO_4^{3-}. The IR peak appearing at 611 cm^{-1} is assigned to the vibrations of OH^- for the adsorbed water molecules.[22,23] The IR spectra of the CHAPF show that all bands present moderate intensities compared to that of CHAP. The frequencies of most remaining bands have changed slightly. This is attributed to changes in the structure that are a result of the calcinations.

pH_{PZC}. The point of zero charge (pH_{PZC}) is defined as the pH at which the total surface charges become zero. The values obtained for the two samples are 7.52 for CHAP and 7.68 for CHAPF. The negligible difference between these two values can be explained by the presence of a specific sorption process and thus the existence of impurities on the powders due to the conditions of the preparation.

Effect of Contact Time. The effect of contact time on the removal of Pb^{2+} by CHAPF at an initial concentration of lead ($C_0 = (20, 50, 100, 200, 500,$ and $700)$ mg·L^{-1}) and for sorbent dosage ($m = 1$ g·L^{-1}) showed rapid adsorption of Pb^{2+} in the first 10 min; thereafter, the adsorption rate decreased gradually, and the adsorption reached an equilibrium in about 30 min as shown in Figure 3. An increase in contact time up to 1 h showed that the Pb^{2+} removal by CHAPF increased by only about 1 % over that obtained at a 30 min contact time. Aggregation of

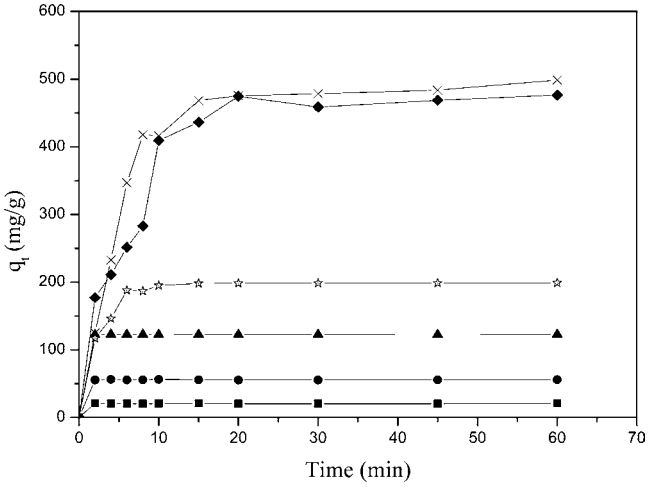

Figure 3. Effect of contact time on lead adsorption by CHAPF at given conditions: pH = 3, dosage = 1 g·L^{-1} at 25 °C. Squares, 20 mg·L^{-1}; circles, 50 mg·L^{-1}; triangles, 100 mg·L^{-1}; stars, 200 mg·L^{-1}; diamonds, 500 mg·L^{-1}; and crosses, 700 mg·L^{-1}.

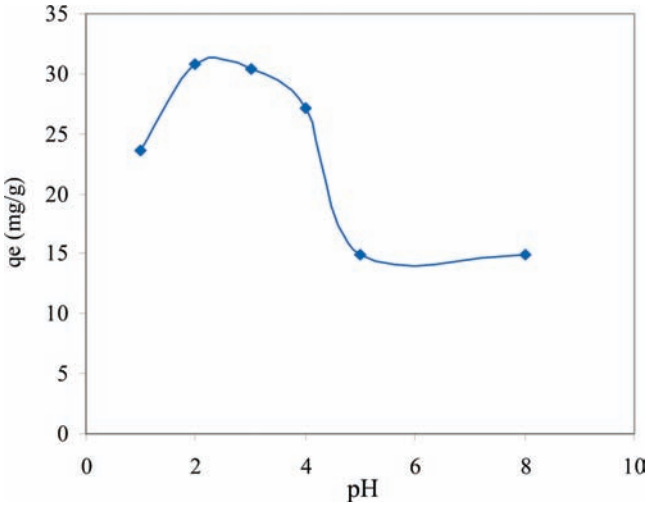

Figure 4. Effect of pH on the lead sorption by CHAPF at given conditions: C_0 = 100 mg·L^{-1}, dosage = 1 g·L^{-1}, contact time = 1 h at 25 °C.

Pb^{2+} ions with the increase in contact time makes it almost impossible for the Pb^{2+} ions to diffuse deeper into the adsorbent structure at the highest energy sites. The adsorption curves were single, smooth, and continuous, leading to saturation, and indicated the possible monolayer coverage on the surface of the adsorbent by the Pb^{2+} ions.

Effect of the pH. The effect of pH on adsorption of Pb^{2+} onto the biosorbent was investigated by varying the solution pH from 1 to 8. The solution pH was adjusted with strong acid (HNO_3) and/or strong base (NaOH) and recorded with a pH meter.

Earlier studies have shown that solution pH is an important parameter influencing the biosorption of metal ions.[24] The removal of Pb^{2+} ions was investigated as a function of solution pH, and the result is indicated in Figure 4. As seen from this figure, the biosorption of Pb^{2+} onto CHAPF is strongly pH dependent. The optimum uptake occurred when the initial pH was 2 and 3 when 99 % of the Pb^{2+} was removed from solution. When the pH passed over 3, the removal efficiency decreased slightly as pH increased, possibly caused by the formation of soluble hydroxyl complexes.[21] These results are in good agreement with the results of previous studies.[24,25]

Kinetic Studies. To analyze the adsorption rates of Pb^{2+} ions onto CHAPF, the experimental data were tested with a pseudo-second-order equation. The kinetic rate linearized equation is expressed as[25]

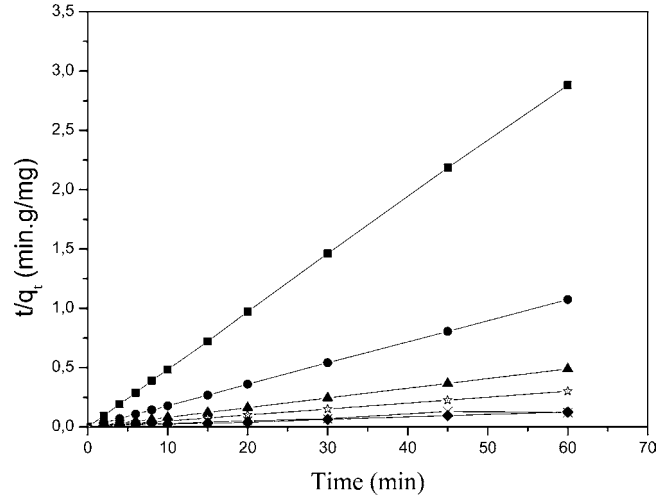

Figure 5. Test of pseudo-second-order model for the adsorption lead on the CHAPF at given conditions (T = 25 °C, ω = 100 rpm, pH = 3, dosage = 1 g·L^{-1}, and time = 1 h). Squares, 20 mg·L^{-1}; circles, 50 mg·L^{-1}; triangles, 100 mg·L^{-1}; stars, 200 mg·L^{-1}; diamonds, 500 mg·L^{-1}; and crosses, 700 mg·L^{-1}.

Table 1. Pseudo-Second-Order Parameters for the Adsorption Lead on CHAPF at 25 °C

C_0 (mg·L^{-1})	K_2 (min^{-1})	R^2	$q_{e,cal}$ (mg·g^{-1})	$q_{e,exp}$ (mg·g^{-1})
20	0.768	0.999	20.833	20.828
50	0.033	0.992	40.983	55.859
100	0.007	1.000	121.951	122.593
200	0.006	0.999	204.081	198.953
500	0.000	0.984	526.315	476.562
700	0.000	0.946	454.545	493.750

$$\frac{t}{q_t} = \frac{1}{K_2 q_e^2} + \frac{1}{q_e} t \qquad (4)$$

where t is the contact time (min); q_t and q_e are the amount of Pb^{2+} removed at an arbitrary time and at equilibrium (mg·g^{-1}), respectively; and K_2 is the rate constant (g·mg^{-1}·min^{-1}). Plots of t/q_t versus t for the removal kinetics of Pb^{2+} ions by the CHAPF are shown in Figure 5.

The $q_{e,exp}$ and the $q_{e,cal}$ values for the pseudo-second-order model are also shown in Table 1. The $q_{e,exp}$ and the $q_{e,cal}$ values are very close to each other, and also, the calculated coefficients of determination, R^2, are close to unity.

On the basis of the regression coefficient and calculated values of adsorption capacity, the adsorption process was found to obey the pseudo-second-order kinetic model.

Adsorption Isotherm. The adsorption isotherms of lead adsorption on CHAPF at various temperatures are depicted in Figure 6. According to the shapes of the curves, the isotherms corresponding to lead adsorption onto CHAPF may be classified as L type of the Giles classification.[26] The L type isotherm suggests a relatively high affinity between lead ions and CHAPF. This also indicates that no strong competition occurs for the adsorption sites between solvent molecules and adsorbate molecules.

The adsorption isotherm study was carried out using two isotherm models: Langmuir and Freundlich isotherm models.

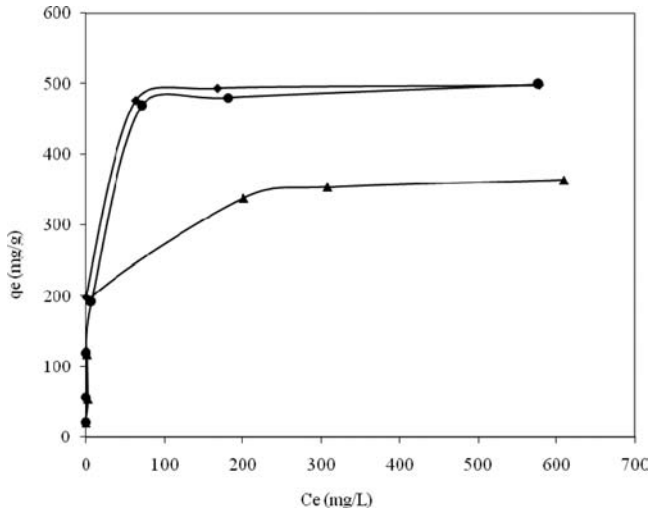

Figure 6. Adsorption isotherms of lead over CHAPF at different temperatures. Diamonds, 25 °C; circles, 35 °C; and triangles, 50 °C (ω = 100 rpm, pH = 3, dosage = 1 g·L^{-1}, and time =1 h).

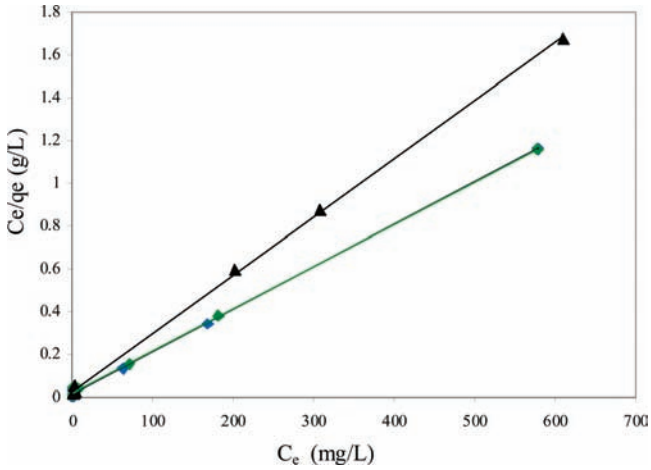

Figure 7. Langmuir adsorption isotherm of lead onto CHAPF for several temperatures: diamonds, 25 °C; circles, 35 °C; and triangles, 50 °C (ω = 100 rpm, pH = 3, dosage = 1 g·L^{-1}, and time =1 h).

The applicability of the isotherm models to the adsorption study data was compared by judging the coefficients of determination, R^2 values.

Langmuir Isotherm. The Langmuir isotherm assumes monolayer adsorption onto a surface containing a finite number of adsorption sites of uniform adsorption with no transmigration of adsorbate in the plane of the surface.[27] The linear form of the Langmuir isotherm equation is given as

$$\frac{C_e}{q_e} = \frac{1}{q_m}C_e + \frac{1}{q_m K_L} \quad (5)$$

where C_e is the equilibrium concentration of the adsorbate (mg·L^{-1}); q_e is the amount of adsorbate adsorbed per unit mass of adsorbent (mg·g^{-1}); and q_m and K_L are Langmuir constants related to adsorption capacity and rate of adsorption, respectively.

When C_e/q_e was plotted against C_e, a straight line with slope of $1/q_m$ was obtained, as shown in Figure 7. An R^2 value of 0.999 indicated that the adsorption data of lead onto the CHAPF at all the three temperatures studied were best fit to the Langmuir isotherm model. The Langmuir constants K_L and q_m were calculated from eq 5, and their values are shown in Table 2.

Table 2. Isotherm Parameters at Various Temperatures for Two Isotherm Models

	Langmuir model			Freundlich model		
temperature	q_m	K_L		K_F		
(°C)	(mg·g^{-1})	(L·mg^{-1})	R^2	(L·mg^{-1})	1/n	R^2
25	500	0.206	0.999	99.174	0.286	0.584
35	500	0.110	0.999	68.469	0.365	0.751
50	370.370	0.111	0.999	56.937	0.328	0.802

Freundlich Isotherm. The Freundlich isotherm on the other hand assumes heterogeneous surface energies, in which the energy term in the Langmuir equation varies as a function of the surface coverage.[28] The well-known logarithmic form of Freundlich isotherm is given by the following equation

$$\ln q_e = \ln K_F + n \ln C_e \quad (6)$$

where C_e is the equilibrium concentration of the adsorbate (mg·L^{-1}); q_e is the amount of adsorbate adsorbed per unit mass of adsorbent (mg·g^{-1}); K_F and n are Freundlich constants with n giving an indication of how favorable the adsorption process is; and K_F (L·mg^{-1}) is the adsorption capacity of the adsorbent. K_F can be defined as the adsorption or distribution coefficient and represents the quantity of lead adsorbed onto CHAPF for a unit equilibrium concentration. The constant n is the empirical parameter related to the intensity of adsorption, which varies with the heterogeneity of the material. When $1/n$ values are in the range $0.1 < 1/n < 1$, the adsorption process is favorable.[29]

The values of K_F were (99.174, 68.469, and 56.937) L·mg^{-1} at (25, 35, and 50) °C, respectively (Table 2). The decrease of K_F with an increase in the temperature revealed that the adsorption capacity of lead onto CHAPF powders increased with a decrease in temperature. Like K_F, n decreased with an increase in temperature, and this represents favorable adsorption at low temperature. If n is below one, then the adsorption is a chemical process; otherwise, the adsorption is a physical process.[30] All values of n exceed one, indicating a favorable adsorption of lead onto CHAPF.

Lead Removal Mechanism. Mechanisms such as ion exchange,[31] surface complexation,[31] dissolution of hydroxyapatite, precipitation of metal phosphate,[32,33] and substitution of Ca in hydroxyapatite by metal during recrystallization (coprecipitation)[34] have been proposed to describe the uptake of heavy metals from aqueous solution by hydroxyapatite.

To investigate the reaction capable of removing lead from the solutions, the evolution of the pH_{Final} according to the contact time was investigated at various initial concentrations of lead and constant values of initial pH (pH = 3) and adsorbent dose (1 g·L^{-1}). The results are presented in Figure 8.

Figure 8 reveals two domains of variation. From the concentration range [(20 to 200) mg·L^{-1}], the pH_{Final} increases from 5 to 6, whereas when the concentration passed over 200 mg·L^{-1}, the pH_{Final} increased slightly. Therefore, the pH_{Final} increase will be induced by H^+ consumption and dissolution of the hydroxyapatite to the $H_2PO_4^-$ species described by eq 7 and precipitation of lead apatites, namely, hydroxypyromorphite,[35] according to eq 8. As both low pH and the presence of Pb^{2+} ions accelerate hydroxyapatite dissolution and formation of $H_2PO_4^-$, in the range pH < 7, $H_2PO_4^-$ is the dominant phosphate species.

$$Ca_{10}(PO_4)_6(OH)_2 + 14H^+ \rightarrow 10Ca^{2+} + 6H_2PO_4 + 2H_2O \quad (7)$$

$$10Pb^{2+} + 6H_2PO_4 + 2H_2O \rightarrow Pb_{10}(PO_4)_6(OH)_2 + 14H^+ \quad (8)$$

For the higher concentration, there are two stages capable of removing lead from the solutions. The first stage is the adsorption of Pb^{2+} on the surfaces of hydroxyapatite, followed by the second stage, an ion exchange reaction between Pb^{2+} adsorbed and Ca^{2+} of CHAPF. The ion exchange interaction can be presented as follows[36]

$$Ca_{10}(PO_4)_6(OH)_2 + xPb^{2+} \rightarrow Pb_xCa_{(10-x)}(PO_4)_6(OH)_2 + xCa^{2+} \quad (9)$$

Wu et al.[37] showed that when $pH < pH_{PZC}$, (P)−OH are the significant surface species, whereas at a pH close to and higher than the pH_{PZC}, the dominant surface species are (P)−O^- and Ca−$(OH)_2^+$, respectively. Our pH_{Final} values < pH_{PZC} suggest that (P)−OH should be the dominant surface species. Therefore, the surface complexation reaction can contribute to a removal of lead by the following general reaction

$$(P)-OH + Pb^{2+} \rightarrow (P)-O-Pb^+ + H^+ \quad (10)$$

The complexation of Pb^{2+} on the CHAPF surface displaced partially the H^+ ions,[37] giving a pH decrease. However, Figure 8 does not reveal any decrease in the pH_{Final} values. Consequently, the probability of the contribution of the surface complexation mechanism is small in our case.

Finally, the surface precipitation mechanism, accompanied generally by the absence of a saturation stage,[38] was also withdrawn because the result obtained by the Langmuir model indicates the monolayer adsorption of lead onto CHAPF. In addition, the observation of equilibrium sorption after a few minutes confirmed the absence of a surface precipitation process for the reason that the coprecipitates of heavy metals are possible only at long-term contacts as indicated by Sposito.[38]

Thermodynamic Studies. Thermodynamic parameters such as Gibbs energy change ($\Delta G°$), enthalpy change ($\Delta H°$), and

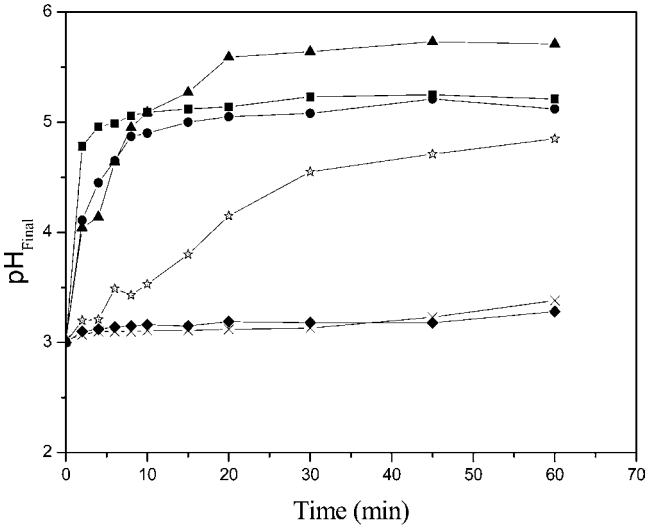

Figure 8. Evolution of the pH_{Final} with time at various concentration of lead. Squares, 20 mg·L^{-1}; circles, 50 mg·L^{-1}; triangles, 100 mg·L^{-1}; stars, 200 mg·L^{-1}; diamonds, 500 mg·L^{-1}; and crosses, 700 mg·L^{-1} (ω = 100 rpm, pH = 3, dosage = 1 g·L^{-1}, and time = 1 h).

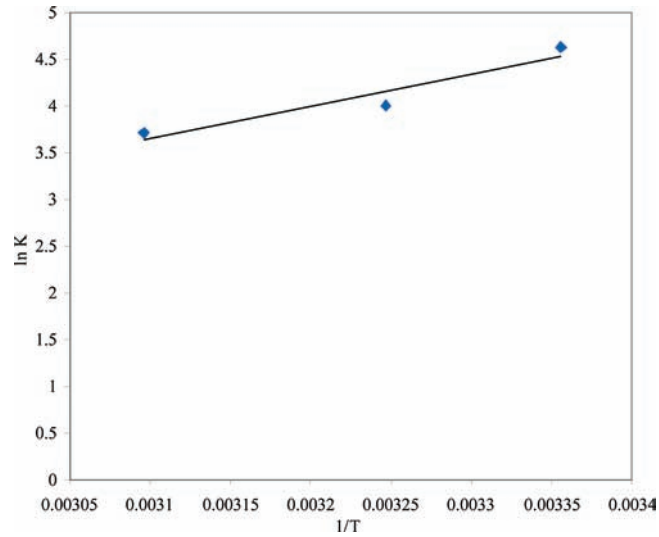

Figure 9. Enthalpy determination curves for the sorption of lead onto CHAPF.

Table 3. Thermodynamic Parameters for Sorption of Pb^{2+} onto CHAPF

temperature (K)	K (L·g^{-1})	$\Delta G°$ (kJ·mol^{-1})	$\Delta S°$ (kJ·mol^{-1})	$\Delta H°$ (kJ·mol^{-1})	R^2
298	103	−36.985			
308	55	−37.537	0.029	−28.575	0.912
323	41.111	−37.974			

entropy change ($\Delta S°$) for the sorption of Pb^{2+} on CHAPF were determined using the following equations[39]

$$\Delta G° = -RT \ln K \quad (11)$$

$$\ln K = \Delta H° - T\Delta S° \quad (12)$$

where $\Delta G°$ is the change in Gibbs energy (kJ·mol^{-1}); $\Delta H°$ is the change in enthalpy (kJ·mol^{-1}); $\Delta S°$ is the change in entropy (J·mol^{-1}·K^{-1}); T is the absolute temperature in kelvin; R is the gas constant; and K is the equilibrium constant of sorption. Equations 11 and 12, can be rewritten as

$$\ln K = \left(\frac{\Delta S°}{R}\right) - \left(\frac{\Delta H°}{RT}\right) \quad (13)$$

$\Delta H°$ and $\Delta S°$ values for lead sorption can be evaluated from the slope and intercept of the linear plot ln K vs $1/T$ (Figure 9, Table 3).

Negative values of the Gibbs energy ($\Delta G°$) indicate the feasibility and spontaneous nature of the lead sorption process, while the negative value of the enthalpy ($\Delta H°$) suggests the exothermic nature of the sorption of Pb^{2+} on CHAPF. We notice that the Gibbs energy ($\Delta G°$) is very close for the three temperatures which means that the temperature 25 °C is more favorable for the sorption of lead. A positive entropy of sorption also reflects the affinity of the sorbent for Pb^{2+}.

Conclusion

This study shows that the carbonate hydroxyapatite prepared from egg shell (CHAPF) represents the highest capacity for adsorption of Pb^{2+} ions from aqueous solution. It has been found that the initial rate of adsorption was high. The sorption isotherms follow the model of Langmuir with high adsorption

capacities and low temperature dependency. The thermodynamic functions were calculated, and it can be concluded that the adsorption of Pb^{2+} over CHAPF is an exothermic and spontaneous process.

The adsorption was greatly pH dependent, with a high uptake of lead at pH = 3. These results show that the lead uptake by CHAPF was very sensitive to the initial concentration of Pb^{2+} in aqueous solution. The study revealed that the mechanism of dissolution of CHAPF and precipitation of hydrophyromorphite was dominant at low concentrations of Pb^{2+} [(20 to 200) $mg \cdot L^{-1}$]. For the high concentrations [(500 to 700) $mg \cdot L^{-1}$], two stages were observed: adsorption of Pb^{2+} ions on the CHAPF surface and an ion exchange reaction between Ca^{2+} of CHAPF and Pb^{2+} ions in aqueous solution.

Literature Cited

(1) Baptista Neto, J. A.; Smith, B. J.; McAllister, J. J. Heavy metal concentrations in surface sediments in a near shore environment, Jurujuba Sound, Southeast Brazil. *Environ. Pollut.* **2000**, *109*, 1–9.

(2) Zhuang, P.; Zou, H.; Shu, W. Biotransfer of heavy metals along a soil-plant-insect-chicken food chain: Field study. *J. Environ. Sci.* **2009**, *21*, 849–853.

(3) Ahamed, M.; Verma, S.; Kumar, A.; Siddiqui, M. K. J. Environmental exposure to lead and its correlation with biochemical indices in children. *Sci. Total Environ.* **2005**, *346*, 48–55.

(4) Esalah, J. O.; Weber, M. E.; Vera, J. H. Removal of lead from aqueous solutions by precipitation with sodium di-(n-octyl) phosphinate. *Sep. Purif. Technol.* **2000**, *18*, 25–36.

(5) Juang, R. S.; Shiau, R. Ch. Metal removal from aqueous solutions using chitosan-enhanced membrane filtration. *J. Membr. Sci.* **2000**, *165*, 159–167.

(6) Ahmed, S.; Chughtai, Sh.; Keane, M. A. The removal of cadmium and lead from aqueous solution by ion exchange with Na-Y zeolite. *Sep. Purif. Technol.* **1998**, *13*, 57–64.

(7) Meunier, N.; Blais, J. F.; Tyagi, R. D. Removal of heavy metals from acid soil leachate using cocoa shells in a batch counter-current sorption process. *Hydrometallurgy* **2004**, *73*, 225–235.

(8) Martinez-Garcia, G. R.; Bachmann, Th.; Williams, C. J.; Burgoyne, A.; Edyvean, R. G. J. Olive oil waste as a biosorbent for heavy metals. *Int. Biodeterior. Biodegrad.* **2006**, *58*, 231–238.

(9) Saeed, A.; Akhter, M. W.; Iqbal, M. Removal and recovery of heavy metals from aqueous solution using papaya wood as a new biosorbent. *Sep. Purif. Technol.* **2005**, *45*, 25–31.

(10) Reza Sangi, M.; Shahmoradi, A.; Zolgharnein, J.; Azimi, Gh. H.; Ghorbandoost, M. Removal and recovery of heavy metals from aqueous solution using Ulmus carpinifolia and Fraxinus excelsior tree leaves. *J. Hazard. Mater.* **2008**, *155*, 513–522.

(11) Dupoirieux, L.; Plane, L.; Gard, C.; Penneau, M. Anatomical basis and results of the facial artery musculomucosal flap for oral reconstruction. *Br. J. Oral Maxillofacial Surg.* **1999**, *37*, 25–28.

(12) Sevgi Ozyegin, L.; Oktar, F. N.; Gultekin Goller, E.; Kayali, S.; Yazici, T. Plasma-sprayed bovine hydroxyapatite coatings. *Mater. Lett.* **2004**, *58*, 2605–2609.

(13) Al-Asheh, S.; Banat, F.; Mohai, F. Sorption of copper and nickel by spent animal bones. *Chemosphere* **1999**, *39*, 2087–2096.

(14) Hassan, S. S. M.; Awwad, N. S.; Aboterika, A. H. A. Removal of mercury(II) from wastewater using camel bone charcoal. *J. Hazard. Mater.* **2008**, *154*, 992–997.

(15) Ye, Xu.; Dazhi, W.; Yang, L.; Tang, H. Hydrothermal conversion of coral into hydroxyapatite. *Mater. Charact.* **2001**, *47*, 83–87.

(16) Wei, Z.; Xiao-ming, Li.; Qi, Y.; Guang-ming, Z.; Xiang-xin, S.; Ying, Z.; Jing-jin, L. Adsorption of Cd(II) and Cu(II) from aqueous solution by carbonate hydroxylapatite derived from eggshell waste. *J. Hazard. Mater.* **2007**, *147*, 534–539.

(17) Dexiang, L.; Wei, Z.; Xiaoming, L.; Qi, Y.; Xiu, Y.; Liang, G.; Guangming, Z. Removal of lead (II) from aqueous solutions using carbonate hydroxyapatite extracted from eggshell waste. *J. Hazard. Mater.* **2010**, *177*, 126–130.

(18) Bell, L. C.; Posner, A. M.; Quirk, J. P. The point of zero charge of hydroxyapatite and fluorapatite in aqueous solutions. *J. Colloid Interface Sci.* **1973**, *42*, 250–261.

(19) Joschek, S.; Nies, B.; Krotz, R.; Gopferich, A. Chemical and physicochemical characterization of porous hydroxyapatite ceramics made of natural bone. *Biomaterials* **2000**, *21*, 1645–1658.

(20) Landi, E.; Tampieri, A.; Celotti, G.; Langenati, R.; Sandri, M.; Sprio, S. Nucleation of biomimetic apatite in synthetic body fluids: dense and porous scaffold development. *Biomaterials* **2005**, *26*, 2835–2845.

(21) Corami, A.; Mignardi, S.; Ferrini, V. Cadmium removal from single- and multi-metal (Cd+Pb+Zn+Cu) solutions by sorption on hydroxyapatite. *J. Colloid Interface Sci.* **2008**, *317*, 402–408.

(22) Purevsuren, B.; Avid, B.; Gerelmaa, T.; Davaajav, Ya.; Morgan, T. J.; Herod, A.; Kandiyoti, R. The characterization of tar from the pyrolysis of animal bones. *Fuel* **2004**, *83*, 799–805.

(23) Raynaud, S.; Champion, E.; Bernache-Assollant, D.; Thomas, P. Calcium phosphate apatites with variable Ca/P atomic ratio I. Synthesis, characterization and thermal stability of powders. *Biomaterials* **2002**, *23*, 1065–1072.

(24) Gupta, V. K.; Shrivastava, A. K.; Neeraj, J. Biosorption of Chromium (VI) From Aqueous solutions by green algae spirogyra species. *Water Res.* **2001**, *35*, 4079–4085.

(25) Ho, Y. S.; McKay, G. A. Kinetic study of dye sorption by biosorbent waste product pith. *Resour. Conserv. Recycl.* **1999**, *25*, 171–193.

(26) Dabrowski, A.; Podkoscielny, P.; Hubicki, Z.; Barczak, M. Adsorption of phenolic compounds by activated carbon- a critical review. *Chemosphere* **2005**, *58*, 1049–1070.

(27) Rengaraj, S.; Kim, Y.; Kyun, Ch.; Jongheop, Joo. Removal of copper from aqueous solution by aminated and protonated mesoporous aluminas: kinetics and equilibrium. *J. Colloid Interface Sci.* **2004**, *273*, 14–21.

(28) Allen, S. J.; Gan, Q.; Matthews, R.; Johnson, P. A. Comparison of optimized isotherm models for basic dye adsorption by kudzu. *Bioresour. Technol.* **2003**, *88*, 143–152.

(29) Khezami, L.; Chetouani, A.; Taouk, B.; Capart, R. Production and characterization of activated carbon from wood components in powder cellulose, lignia, xylan. *Powder Technol.* **2005**, *157*, 48–56.

(30) Yeddou Mezenner, N.; Bensmaili, A. Kinetics and thermodynamic study of phosphate adsorption on iron hydroxide-eggshell waste. *Chem. Eng. J.* **2009**, *147*, 87–96.

(31) Corami, A.; Mignardi, S.; Ferrini, V. Copper and zinc decontamination from single- and binary-metal solutions using hydroxyapatite. *J. Hazard. Mater.* **2007**, *146*, 164–170.

(32) Deydier, E.; Guilet, R.; Sharrock, P. Beneficial use of meat and bone meal combustion residue: "an efficient low cost material to remove lead from aqueous effluent. *J. Hazard. Mater.* **2003**, *101*, 55–64.

(33) Yuping, Xu.; Schwartz, F. W. Lead immobilization by hydroxyapatite in aqueous solutions. *J. Contam. Hydrol.* **1994**, *15*, 187–206.

(34) Yuping, Xu.; Schwartz, F. W.; Traina, S. J. Sorption of Zn^{2+} and Cd^{2+} on Hydroxyapatite Surfaces. *Environ. Sci. Technol.* **1994**, *28*, 1472–1480.[2]

(35) Baillez, S.; Nzihou, A.; Bernache-Assolant, D.; Champion, E.; Sharrock, P. Removal of aqueous lead ions by hydroxyapatites: Equilibria and kinetic processes. *J. Hazard. Mater.* **2007**, *139*, 443–446.

(36) HuanYan, X.; Lei, Y.; Peng, W.; Yu, L.; MingSheng, P. Kinetic research on the sorption of aqueous lead by synthetic carbonate hydroxyapatite. *J. Environ. Manage.* **2008**, *86*, 319–328.

(37) Wu, L.; Forsling, W.; Schindler, P. W. Surface complexation of calcium minerals in aqueous solution: 1.Surface protonation at fluorapatite—water interfaces. *J. Colloid Interface Sci.* **1991**, *147*, 178–185.

(38) Sposito, G. Distinguishing adsorption from surface precipitation. *ACS Symp. Ser.* **1986**, *323*, 217–228.

(39) Jiang, J. Q.; Cooper, C.; Ouki, S. Comparison of modified montmorillonite adsorbents. Part I. Preparation, characterization and phenol adsorption. *Chemosphere* **2002**, *47*, 711–716.

Received for review December 19, 2009. Accepted June 13, 2010.

JE901070E